ESTABLISHMENT OF CENTRELINE TEMPERATURES IN IRRADIATED NUCLEAR FUELS

E.N. ONDER, S. YATABE and D. ROUBTSOV
Canadian Nuclear Laboratories
286 Plant Road, Chalk River, Ontario, K0J 1J0 - Canada

ABSTRACT

High temperature promotes the mobility of UO_2 grain boundaries, resulting in grain growth. Therefore, grain growth, based on pre- and post-irradiation grain size measurements, can be used to estimate the in-reactor temperature of UO_2 fuel. Using models based on grain growth, fuel temperatures can be estimated for irradiated fuels. Temperatures can also be calculated using models based on thermal conductivity, element linear power, and fuel burnup. The consistency of the models can be verified by comparing the calculated centreline fuel temperatures with those estimated from measured grain sizes. The objective of this work is to assess the consistency of the models that are used in fuel performance codes. Model parameters (*e.g.*, irradiated fuel grain size, linear power) obtained from the Canadian Nuclear Laboratories database are used to establish fuel centerline temperatures using different models. Then the fuel centerline temperatures, obtained in different ways, are compared for consistency.

1. Introduction

Understanding and establishing fuel behaviour and performance parameters are essential to the design of nuclear fuels and to the development and validation of fuel models and codes, which in turn ensure fuel efficiency and safety. Empirical models are usually developed to be employed in fuel performance codes. From the standpoint of validation and verification of nuclear engineering modeling tools (codes), it is important to verify the models independently from the codes, and to verify the consistency of the parameters used in the models with available experimental data. It is well-known that fuel behaviour can be established through destructive and non-destructive Post-Irradiation Examination (PIE) of fuels obtained from power and research reactors.

Based on PIE performed at Canadian Nuclear Laboratory (CNL), a fuel performance database has been assembled. Fuel performance parameters, such as grain size and element power history, obtained from this database can be used to establish fuel centerline temperatures using different models/methods.

Employing the models based on grain growth (using pre- and post-irradiation grain size measurements), fuel temperatures can be estimated for irradiated fuels. Fuel temperature can also be calculated using the models based on fuel pin (element) thermal conductivity, element linear power, and burnup. The linear power and burnup are based on the power history data recovered from irradiation reports and are incorporated into the CNL database. Consequently, the consistency of the models can be verified by comparing the calculated centreline fuel temperatures with those estimated from measured grain sizes.

2. Description of Fuel for Fuel Performance Analysis

This study focuses on the behaviour of fuel bundles used in heavy water-cooled, CANDU-type nuclear reactors. All examined CANDU[1] bundles were fabricated based on sintered natural uranium UO_2, consist of 37 elements with split spacers to provide enough spacing between elements, bearing pads to ensure enough spacing between the bundle and the pressure tube, and endplates to hold the elements together as a fuel assembly. The bundle length is ~0.5m.

[1] CANDU® (CANada Deuterium Uranium) is a registered trademark of AECL.

Four bundles have been analysed for this study. Two bundles were manufactured to meet the design specifications of standard CANDU-6 (37-element natural uranium UO_2) fuel. PIE results [1] obtained for elements with CANLUB (CANada LUBricant), a carbon-based coating applied to the inner surface of the fuel sheath to protect it from stress corrosion cracking [2] are used for this study to provide reference values to the other bundles that are discussed here. These two bundles with CANLUB coated elements, *hereafter called the standard bundles,* have the same features as regular CANDU bundles. One of the bundles (standard bundle 1) achieved a calculated bundle-average burnup of 199 MWh/kgU (8.3 MWd/kgU), and an outer element linear power (OELP)[2] of 47 kW/m. This peak linear power in the outer ring element was achieved at an element burnup of 88 MWh/kgU, or 3.6 MWd/kgU at bundle 7 location from the channel inlet. The other fuel bundle (standard bundle 2) achieved a calculated bundle-average burnup of 202 MWh/kgU (8.4 MWd/kgU), and a peak OELP[3] of 48 kW/m. This peak linear power in the outer ring element was achieved at an element burnup of 45 MWh/kgU, or 1.9 MWd/kgU at bundle 7 location from the channel inlet.

In addition, two CANDU-type bundles discharged at extended burnups, *hereafter called the extended burnup or high-burnup (bundles)*, were also analysed. One of the high-burnup bundles (high-burnup bundle 1) achieved a calculated bundle-average burnup of 409 MWh/kgU (17 MWd/kgU) and OELP[4] of 47 kW/m. This peak linear power in the outer ring element was achieved at an element burnup of 55 MWh/kgU, or 2.3 MWd/kgU at bundle 9 location from the inlet. The other bundle (high-burnup bundle 2) achieved a calculated bundle-average burnup of 492 MWh/kgU (21 MWd/kgU), and OELP[5] of 41 kW/m. This peak linear power in the outer ring element was achieved at an element burnup of 27 MWh/kgU, or 1.1 MWd/kgU at bundle 8 location from the channel inlet.

3. Analysis

3.1 Establishment of Fuel Temperatures

Estimates of fuel temperatures are based on the usage of two different techniques to independently verify the consistency of obtained results. The first method is to calculate the fuel temperature using the thermal conductivity integral and the second approach is to apply the temperature dependent grain growth models. These methods and the comparison of the obtained fuel temperature predictions will be discussed in detail in the following sections. It should be noted that different assumptions may be made while applying different techniques/methods, which in turn can have effects on the centreline temperature estimates obtained from using the different methods. In this analysis, the peak powers and corresponding burnups are used to estimate the maximum temperatures.

3.1.1 Estimation of Fuel Temperature based on Thermal Conductivity Integral

The first approach used to calculate the temperature at the centre of the fuel pellet is to employ the thermal conductivity integral expressed in terms of linear power (q') as

$$\int_{T_s}^{T_{max}} k_f dT = \int_0^{T_{max}} k_f dT - \int_0^{T_s} k_f dT = \frac{q'}{4\pi} \quad (1)$$

where T_{max} is the temperature at the centre of the pellet, T_s is the temperature at the pellet surface and k_f is the thermal conductivity of the fuel.

Temperature at the pellet surface:

The temperature at the pellet surface is calculated using the thermal resistance analogy [3] as follows:

[2] The OELP varied between 47 kW/m and 39 kW/m during the residency in the reactor.

[3] The OELP varied between 48 kW/m and 40 kW/m during the residency in the reactor.

[4] The OELP varied between 47 kW/m and 30 kW/m during the residency in the reactor.

[5] The OELP varied between 41 kW/m and 30 kW/m during the residency in the reactor.

$$T_s - T_b = q' \left[\frac{1}{2\pi R_g h_g} + \frac{1}{2\pi k_{cl}} \ln\left(\frac{R_{clo}}{R_{cli}}\right) + \frac{1}{2\pi R_{clo} h_{co}} \right] \quad (2)$$

where T_b is the bulk coolant temperature, R_g is the mean radius in the gap between fuel and cladding, h_g is the gap conductance, k_{cl} is the thermal conductivity of cladding, R_{clo} is the outer radius of cladding, R_{cli} is the inner radius of cladding, and h_{co} is the coolant heat transfer coefficient. The fuel element outer diameter (OD) of 13.08 mm and sheath thickness of 0.4 mm with the thermal conductivity of Zircaloy cladding, k_{cl}, of 15.5 W m^{-1} K^{-1} at temperatures varying between 295 and 320°C are employed for this analysis.

CANDU fuel cladding is collapsible. Therefore, it can be assumed that cladding and pellet are in direct contact. However, it may also be possible for a gap to occur between pellet and cladding. In the former assumption, the first term in the r.h.s. of Equation (2) is absent. In the later assumption, h_g has two components, one of which is the solid-to-solid contact spots and the other one is conduction, convection and radiation through the medium in the voids between spots. In addition, can vary depending on the gap width, constituents of gas present in the gap, and interfacial roughness of the surfaces of the sheath and pellet. For example, in [4], h_g varying between 0.7 and 1 W/cm^2 °C is indicated for noble gases, such as argon, krypton or xenon, at a temperature of 300°C.

Calculation of bulk fluid temperature T_b is required for the determination of fuel pellet surface temperature. The original thermalhydraulic (TH) conditions in the fuel channels in which the bundles were irradiated are unknown and are set to provide conservative results (*i.e.*, higher coolant temperatures) in this study. Therefore, several different combinations of TH conditions were tested to provide the highest possible fluid temperatures. The following conditions were tested: i) channel powers of 5.5 and 6.0 MW; ii) mass flow rate of 21 and 23 kg/s; iii) inlet coolant temperature of 265°C and 270°C, and iv) system pressure of 10.0 MPa for all cases.

For a simple model of cosine-shape axial power profile in the fuel channel (assuming no perturbation in the vicinity of fuel channel), the axial variation of fluid (bulk) temperature, T_b, with the inlet of fuel channel as the reference point, is given by [3]

$$T_b(z) = T_{in} + \frac{Q}{2\dot{m}c_p}\left(\sin\frac{\pi\left(z-\frac{L}{2}\right)}{L} + 1\right) \quad (3)$$

where T_{in} is the temperature at the fuel channel inlet, Q is the (fuel) channel power, $\dot{m}$ is the mass flow rate, c_p is the average specific heat between inlet and outlet of the fuel channel, z is the axial location of interest (z = 0 at the inlet), and L is the total length of a bundle string of twelve bundles. On the other hand, the TH conditions at the exit of the fuel channel need to be determined to provide conservative but realistic analysis. Some cases have been avoided because the models used for analysis are not applicable (*e.g.*, channel outlet equilibrium thermodynamic quality[6] exceeds 4%). The amount of boiling can be quantified using the equilibrium thermodynamic quality of the coolant, x_{out}, as

$$x_{out} = \frac{H_{out} - H_f}{H_{fg}} \quad (4)$$

where H_f and H_{fg} are the saturated liquid enthalpy and latent heat of vaporization. The enthalpy at the exit of the fuel channel, H_{out}, is calculated as follows:

$$H_{out} - H_{in} = \frac{Q}{\dot{m}} \quad (5)$$

where the inlet enthalpy (H_{in}) is a function of the system pressure and inlet temperature. Boiling in the channel is initiated once enthalpy at any given location exceeds the saturation enthalpy for a given pressure. For all the cases tested (eight, with different combinations of TH conditions as discussed above), the enthalpy at the outlet was higher than the saturation

[6] In CANDU reactors, in order to maximize the thermal efficiency, boiling in the core at high power is permitted, with the equilibrium thermodynamic quality in reactor outlet headers as high as 4% at full power.

enthalpy. For four out of the eight cases, the equilibrium thermodynamic qualities at the exit (x_{out}) were higher than 4%, and those cases were excluded from the analysis. Fluid temperature variations along the fuel channel for the remaining four cases are demonstrated in Figure 1. Of the remaining four cases, the case with the channel power of 5.5 MW, flow rate of 23 kg/s, and inlet coolant temperature of 270°C provides the most conservative result (*i.e.*, it provides higher coolant temperatures across the fuel channel); this case was selected for further analysis.

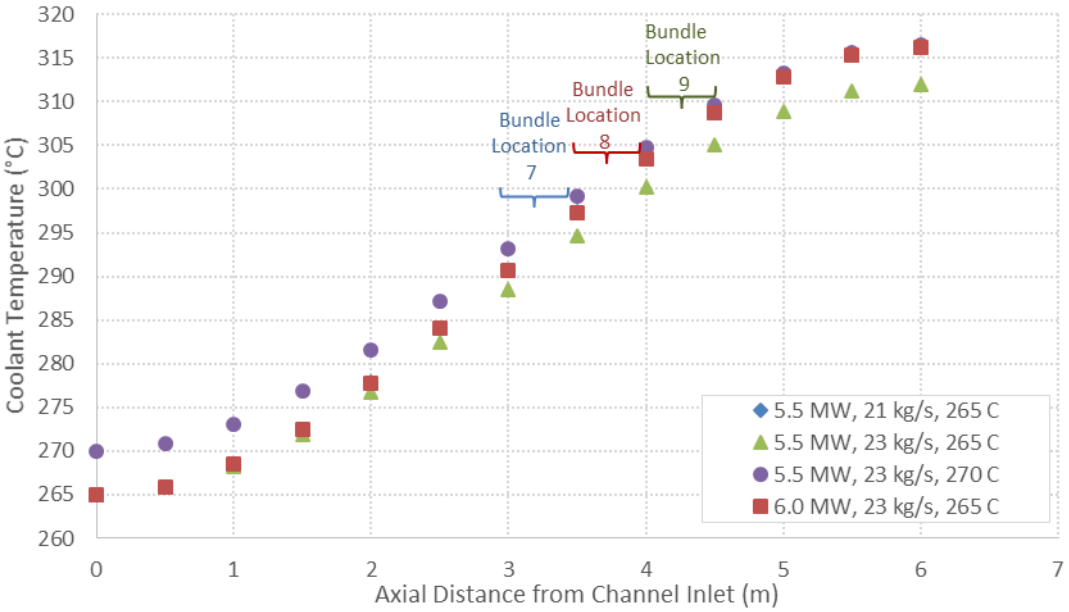

Figure 1: Variation of Fluid Temperature along the Fuel Channel

The cross section average fluid temperatures are calculated depending on the location of the fuel bundle of interest:

- Standard bundle 1 (47 kW/m, 199 MWh/kgU) achieved its peak power and reached its discharge burnup in the fuel channel at bundle position 7: coolant temperature at bundle position 7 is 296°C.
- Standard bundle 2 (48 kW/m, 202 MWh/kgU) achieved its peak power and reached its discharge burnup in the fuel channel at bundle position 7: coolant temperature at bundle position 7 is 296°C
- High burnup bundle 1 (47 kW/m, 409 MWh/kgU) achieved its peak power at bundle location 5, and reached its discharge burnup in the fuel channel at bundle position 9: coolant temperature at bundle location 9 is 307°C
- High burnup bundle 2 (41 kW/m, 492 MWh/kgU) achieved its peak power and reached its discharge burnup in the fuel channel at bundle position 8: coolant temperature at bundle position 8 is 302°C

Figure 2 shows the variation of pellet surface temperature estimated with different gap conductance values. In this figure, pellet surface temperatures without any gap are shown as dotted lines for the four bundles that are analysed in this study. Given that the cladding is collapsible in a CANDU fuel element, it is expected that direct contact between fuel and cladding will be established. In the case of direct contact, without any gap, pellet surface temperatures (~ 350°C) are significantly lower than the cases with the gap. The gap width was assumed to be 10 µm. Despite that, in [4], the recommended values for the gap conductance are between 0.7 and 1 W/cm^2 °C (or 7 and 10 kW/m^2 °C), the larger interval of the possible values of h_g was used to demonstrate the trend as depicted in Figure 2. For this analysis, two different pellet surface temperatures were considered: the first choice corresponds to the case with no gap, and the second one is for a gap of 10 µm width with a

gap conductance of 10 kW/m^2 °C. The case with a finite gap width will lead to more conservative results for the central fuel temperatures.

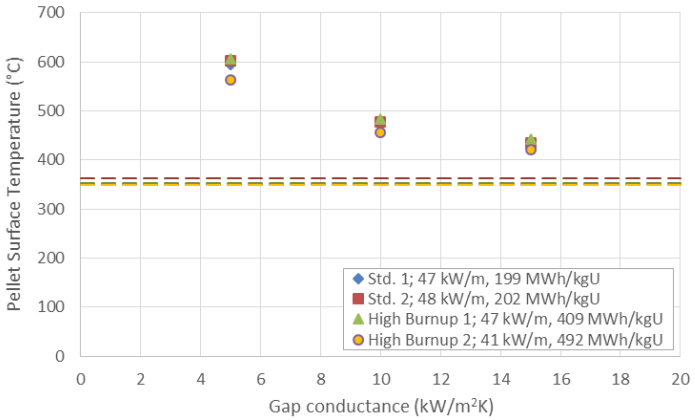

Figure 2: Variation of Pellet Surface Temperature T_s with Gap Conductance h_g

Temperature at the pellet centre:

Based on Equation (1), temperatures at the pellet centre are calculated using the temperatures at the fuel pellet surface and linear power. In the analysis, two thermal conductivity equations are used: the Fink-Lucuta and Halden models. The thermal conductivity equation for 95% theoretical density (TD) developed by Fink [6] and the correction factors (developed by Lucuta et al. [7]) are shown in Table 1. The correction factors are applied to take into account separate effects for fission products and radiation damage. Both models (*i.e.*, Fink-Lucuta and Halden) are recommended in [5] and used as options in the BISON code [8]. The Fink-Lucuta equation with corrections [6], [7] is given in Table 1, where *T* is the temperature in K, *t* is *T*/1000, *p* is the porosity, *Bu* is the burnup in at.%, and the thermal conductivity, *k*, is in W/mK.

Table 1: Fink-Lucuta Equation

Description of Equation	Equation
UO_2 with 95% theoretical density [6]	$k_{95} = \frac{100}{7.5408 + 17.692\,t + 3.6142\,t^2} + \frac{6400}{t^{5/2}} \exp\left(-\frac{16.35}{t}\right)$
UO_2 with 100% theoretical density [5]	$k = k_{100} = k_{95}\left[\frac{1}{1 - 0.05\times(2.6 - 0.5t)}\right]$
Correction Factor – Dissolved Fission Products [7]	$f_d = \left(\frac{1.09}{Bu^{3.265}} + 0.0643\sqrt{\frac{T}{Bu}}\right)\arctan\left(\frac{1.0}{\frac{1.09}{Bu^{3.265}} + 0.0643\sqrt{\frac{T}{Bu}}}\right)$
Correction Factor – Precipitated Fission Products [7]	$f_p = 1.0 + \left(\frac{0.019}{3.0 - 0.019\,Bu}\right)\left(\frac{1.0}{1.0 + \exp\left(-\frac{T - 1200}{100}\right)}\right)$
Correction Factor – Porosity [7]	$f_{por} = \frac{1.0 - p}{1.0 + 0.5\,p}$
Correction Factor – Radiation Damage [7]	$f_r = 1.0 - \frac{0.2}{1.0 + \exp\left(\frac{T - 900}{80}\right)}$

For a given burnup and temperature, the Fink-Lucuta model can be employed to calculate the thermal conductivity of 95%TD and 100%TD and correction factors for dissolved and precipitated fission products as well as for radiation damage. However, the porosity correction factor requires the knowledge of fuel density at a given burnup. The relationship between the density, ρ, and burnup, *bu,* in GWd/tM, is given [9] by

$$\frac{\rho}{\rho_{th}} = 0.963 - 0.0001 \times bu^{3/2} \qquad (6)$$

where ρ_{th} is the theoretical density of UO_2.

The Halden model [10] is given for the 95%TD fuel as follows:

$$k = \frac{1}{0.1148+0.0035\,B+0.0002475\,(1-0.00333\,B)\,T} + 0.0132\exp(0.00188\,T) \quad (7)$$

where B is burnup in MWd/kgUO$_2$, T is in °C, and the thermal conductivity, k, in W/mK. A density correction needs to be applied to calculate the thermal conductivity for the four fuel elements with the densities estimated by Equation (6) for a given element burnup.
Figure 3 shows the thermal conductivities calculated for the standard 1 fuel at a linear power of 47 kW/m and a bundle average discharge burnup of 199 MWh/kgU (an outer element burnup of 225 MWh/kgU, or 9.4 MWd/kgU). In Figure 3, f_t represents the product of all correction factors, f_d, f_p, and f_r.

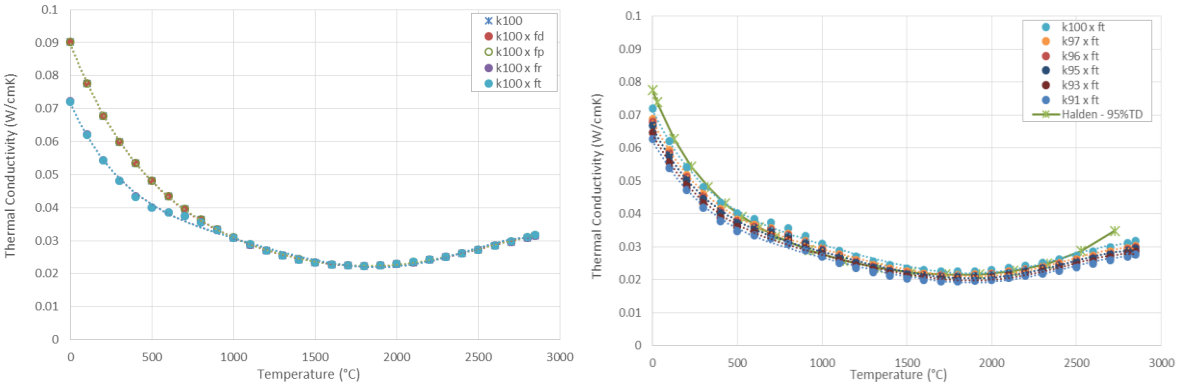

(a) (b)

Figure 3: Comparison of *k(T)* obtained using Fink-Lucuta Thermal Conductivity Equation for: (a) Separate Effects for 100%TD fuel, (b) Effect of Fuel Density (at various %TD) and also with the Halden Model (95%TD) for Standard 1 Fuel

3.1.2 Estimation of Fuel Temperature based on Grain Growth Models

Equiaxed grain growth are observed in the irradiated fuels at the power levels of interest to CANDU reactors. Two models for grain growth are applied in this analysis: i) a model developed by Hastings *et al.* [11], [12] and ii) a model developed by Ainscough *et al.* [13] (and used in the BISON code).

The model of Hastings *et al.* [11], [12] for the equiaxed grain growth is given by

$$D^n - D_o^n = kt\exp\left(-\frac{Q}{RT}\right) \quad (8)$$

where D_o is the original grain size in μm, D is the grain size in μm, the burnup time t is in seconds, the temperature T is in K, n is an exponent, k is the rate constant in μm^n/s, Q is the apparent activation energy in kJ/mol, and R is the gas constant (= 0.008314 kJ/K mol). Based on analysis of CNL experiments, the following values were suggested in [11], [12] for commercially fabricated natural uranium UO$_2$ fuel: n = 2.5, k = 1.3×10^6 μ$^{2.5}$ s^{-1}, and Q = 320 ± 10 kJ/mol. Time t in Equation (8) is calculated based on the element burnup, element power, and uranium mass in the fuel element.

The model of Ainscough *et al*. [13] is given by the following equation on $D(t)$:

$$\frac{dD}{dt} = k\left(\frac{1}{D} - \frac{1}{D_m}\right) \quad (9)$$

Integration of Equation (9) gives the following relation[7]:

$$D_m(D_0 - D) + D_m^2 \ln\left(\frac{D_m - D_0}{D_m - D}\right) = kt \quad (10)$$

[7] A misprint occurs in the original paper [13]: the denominator in the second term (*i.e.*, the term with *ln* function) was given as (D – D$_0$), instead of D$_m$ – D.

where D_m is the limiting grain size in μm, given by

$$D_m = 2230 \exp\left(-\frac{7620}{T}\right) \quad (11)$$

k is the rate constant in μm^2/h, given by

$$k = 5.24 \times 10^7 \exp\left(-\frac{2.67\times10^5}{RT}\right) \quad (12)$$

where R is the gas constant (= 8.314 J/K mol), D_o is the as-fabricated grain size in μm, D is the grain size in μm after the irradiation/burnup time t, in hours, and the temperature T is in K. It is expected that the maximum grain growth is achieved at the highest temperature or at the peak power. Grain growth is affected by time, as well as by fuel temperature. Therefore, grain growth can be calculated using Equation (8) or Equation (10) at the peak power reached by a fuel element at the corresponding burnup interval (*i.e.*, burnup variation at the peak power with power variations within 1 kW/m). It should be noted that in CANDU, the highest power in fuel bundle elements is achieved in the outer ring elements. Within 1 kW/m of linear power variations from the peak linear power, the time t is calculated for a given burnup interval, power, and the mass of uranium. Eqs. (8) and (10) can be considered as algebraic equations to find an unknown T, and T can be interpreted as a fuel centreline temperature T_c. However, iterations are required in (10) for a self-consistent solution.

4. RESULTS

Table 2 shows the parameters used in the models. A density of 96% TD is calculated, using Equation (6), for all fuels corresponding to the burnup at the peak power.

Table 2: Parameters used in the Models

Bundle	Element #	Peak Power (kW/m)	Bundle Average Discharge Burnup MWh/kgU (MWd/kgU)	Element Burnup at the Peak Power, MWh/kgU (MWd/kgU)	Burnup Interval at the Peak Power MWh/kgU (MWd/kgU)	Grain Size after Irradiation (μm)
Standard 1	1	47	199 (8)	111 (5)	16 (1)	15.0
Standard 2	1	48	202 (8)	45 (2)	25 (1)	15.4
Extended Burnup 1	1	47	409 (17)	51 (2)	11 (0)	19.0
	2					18.0
Extended Burnup 2	1	41	492 (21)	248 (10)	14 (1)	11.0
	2					14.0

Figure 4 shows the comparison of fuel centreline temperatures calculated using the Fink-Lucuta model with the correction factors (see Table 1 for the definition of the terms used as correction factors, *i.e.*, k, f_d, f_p, f_{por}, f_r in Figure 4) and the Halden model, using Equation (1) with different pellet-surface temperatures with fuel-cladding gap and no gap conditions. Centreline temperatures for the "no gap" condition are lower than those obtained using the "with gap" condition because direct fuel-pellet contact provides a better heat transfer. The centreline temperature is also tested for fuel elements with other densities ρ. Given that a density of 96%TD was calculated for the burnup of interest, *highlighted in* Figure 4, the variation of fuel centreline temperatures with the density is also verified for Fink-Lucuta and Halden Models. The Fink-Lucuta model predicted slightly higher fuel centreline temperatures for 96%TD than did the Halden model. In addition, the fuel centreline temperatures calculated using the thermal conductivity equations are compared with those obtained from the grain growth models of Hastings *et al*. (see Equation (8)) and Ainscough *et al*. (see Equation (9)). The fuel centreline temperatures derived from grain growth models are similar to and within the range of those obtained from the thermal conductivity equations with the "no gap" condition.

Figure 5 shows the fuel centreline temperatures predicted using different models for the standard fuels (S1 and S2) and extended burnup fuels (EB1 and EB2). The "no gap" condition is used for the models based on the thermal conductivity integrals. In the case of the extended burnup fuels, two elements from the outer rings were examined, whereas for the standard

fuels, only one element from the outer ring was examined[8]. The largest temperature difference (approximately 12%) was observed between Fink-Lucuta and Ainscough models for the standard 2 fuel (S2). Such differences can be expected given that some assumptions were made in the modelling. For instance., burnup interval was used for the calculation of time *t*, and density of the fuel was estimated from Equation (6)).

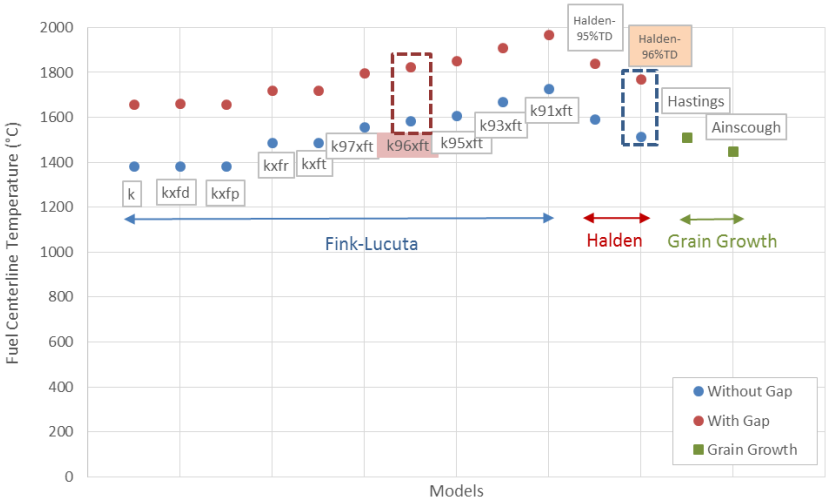

Figure 4: Comparison of Fuel Centreline Temperatures Calculated Using Different Models for Standard 1 fuel

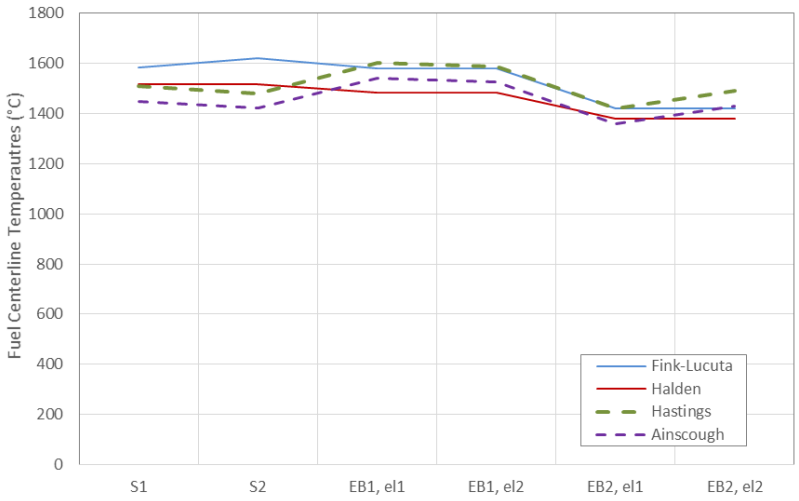

Figure 5: Comparison of Fuel Centreline Temperatures Calculated Using Different Models for Standard (S) and Extended Burnup (EB) Fuels

Figure 6 and Figure 7 show the fuel centreline temperatures predicted using the thermal conductivity equations based on the thermal conductivity integral models and the grain growth models, respectively. For the same conditions, the Fink-Lucuta model systematically predicts the fuel centreline temperatures slightly higher (*i.e.*, by 3-6%) than the Halden model (see Figure 6), and so does the Hastings model compared to Ainscough model (*i.e.*, the Hastings temperature predictions are 4% higher, see Figure 7). These results confirm that fuel centreline temperatures can be consistently predicted using similar concepts (*i.e.*, thermal conductivity integral or grain growth models). In this study, the largest difference was observed between the Fink-Lucuta and Ainscough models. The Halden model more closely matches the grain growth models (Hastings and Ainscough) than does the Fink-Lucuta model, as shown in Figure 8.

[8] Examination means measurement of grain sizes.

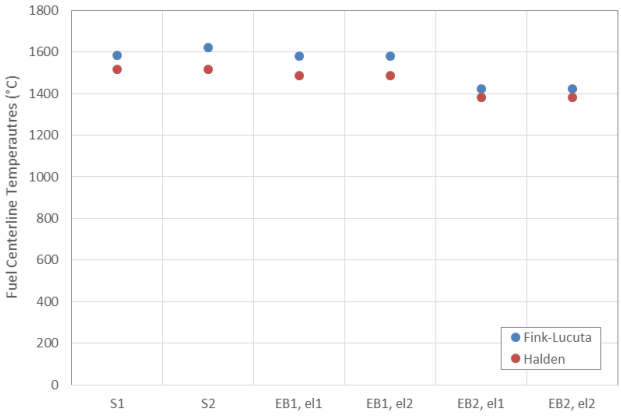

Figure 6: Comparison of Fuel Centreline Temperatures Calculated Using the Thermal Conductivity Integral Model for Standard (S) and Extended Burnup (EB) Fuels

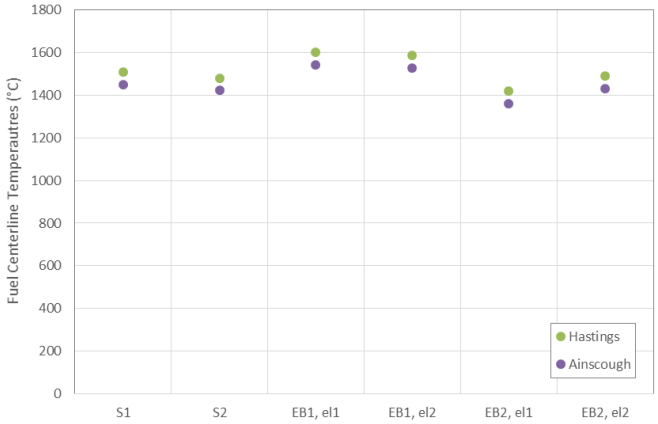

Figure 7: Comparison of Fuel Centreline Temperatures Calculated Using the Grain Growth Models for Standard (S) and Extended Burnup (EB) Fuels

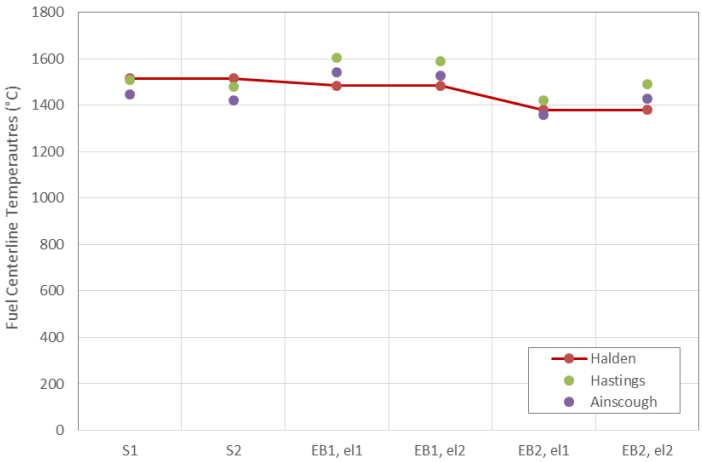

Figure 8: Comparison of Fuel Centreline Temperatures Calculated Using the Halden Model and the Grain Growth Models for Standard (S) and Extended Burnup (EB) Fuels

5. CONCLUSION

Models used in fuel performance codes need to be verified/validated independently for better understanding of their consistency, accuracy, and applicability. However, it is difficult to obtain a sufficient amount of on-line experimental data to verify the models employed in the codes. In this study, the fuel centreline temperatures were calculated using different methods/models and compared for consistency using data obtained from post-irradiation examination (*e.g.*, the grain sizes) and knowledge of the power history from the CNL database. The results have been demonstrated to be consistent within the same approach and

- the Hastings model predicted the fuel centreline temperatures to be consistently higher than the Ainscough model by 4%;
- the Fink-Lucuta model predicted the fuel centreline temperatures to be consistently higher than the Halden model by 3-6%.

Overall, the Fink-Lucuta model predicted higher fuel centreline temperatures than the grain growth models, and the largest difference (up to 12%) in fuel centreline temperatures was observed between the Fink-Lucuta model and the Ainscough model. Fuel centreline temperature predictions of the Halden model are found to be more consistent with those of the grain growth models.

6. REFERENCES

[1] J. Montin, M.R. Floyd, Z. He and E. Kohn, "Performance of Two CANDU-6 Fuel Bundles Containing CANLUB and Non-CANLUB Production Elements", AECL-CONF-1102, presented at the 7th International Conference on CANDU Fuel, Kingston, 2001.

[2] M. Tayal and M. Gacesa, "Chapter 17: Fuel", The Essential CANDU, UNENE, 2014, http://www.nuceng.ca/candu .

[3] B.J. Lewis, E.N. Onder and A.A. Prudil, "Fundamentals of Nuclear Engineering", Wiley, 2017.

[4] A.M. Ross and R.L. Stoute, "Heat Transfer Coefficient between UO_2 and Zircaloy-2", AECL Report AECL-1552, 1962.

[5] IAEA, "Thermophysical Properties Database of Materials for Light Water Reactors and Heavy Water Reactors", IAEA-TECDOC-1496, 2006.

[6] J.K. Fink, "Thermophysical Properties of Uranium Dioxide", J. Nucl. Mater., 279, pp. 1–18, 2000.

[7] P.G. Lucuta, H.J. Matzke, and I.J. Hastings, "A Pragmatic Approach to Modelling Thermal Conductivity of Irradiated UO2 Fuel: Review and Recommendations." J. Nucl. Mater., 232, pp. 166–180, 1996.

[8] J.D. Hales, R.L. Williamson, S.R. Novascone, G. Pastore, B.W. Spencer, D.S. Stafford, K. A. Gamble, D.M. Perez, R.J. Gardner, W. Liu, J. Galloway, C. Matthews, C. Unal, N. Carlson, "BISON Theory Manual", BISON release 1.3, INL/EXT-13-29930 Rev. 3, 2016.

[9] M. Marchetti, D. Laux. L. Fongaro, T. Wiss, P. Van Uffelen, G. Despaux, V.V. Rondinella, "Physical and Mechanical Characterization of Irradiated Uranium Dioxide with a Broad Burnup Range and Different Dopants using Acoustic Microscopy", J. Nucl. Mater., 494, pp. 322–329, 2017.

[10] W. Wiesenack, "Assessment of UO_2 Conductivity Degradation based on In-Pile Temperature Data", Proceedings of 1997 International Topical Meeting on LWR Fuel Performance, Portland, Oregon, March 2-6, 1997.

[11] I.J. Hastings, J.A. Scoberg, and K. MacKenzie, "Grain Growth in UO_2: In-Reactor and Laboratory Testing", J. Nucl. Mater., 82, pp.435, 1979.

[12] I.J. Hastings, J.A. Scoberg, K. MacKenzie, and W. Walden, "Grain Growth in UO_2: Studies at Chalk River Nuclear Laboratories", Atomic Energy of Canada Limited, Report AECL-6411, 1979.

[13] J.B. Ainscough, B.W. Oldfield and J.O. Ware, "Isothermal Grain Growth Kinetics in Sintered UO_2 Pellets", J. Nucl. Mater., 49, pp. 117-128, 1973.

ACKNOWLEDGMENTS

The authors would like to thank Canadian Nuclear Laboratories (CNL) hot cell staff and scientists who were involved in the assessment of nuclear fuel characteristics. This study was funded by Atomic Energy of Canada Limited (AECL).